Journal of Engineering and Computer Sciences
Qassim University, Vol. 7, No. 1, pp. 55-72 (January 2014/Safar 1435H)

Contact Stiffness of Polymer with Nominally Flat Surfaces

Fahad Al-Mufadi
Department of Mechanical Engineering, Engineering College,
Qassim University, Buraidah, KSA
P.O. Box 6677, Buraydah, AlQassim 51452, Saudi Arabia
almufadi @qec.edu.sa

(Received 23/2/2014; accepted for publication 13/4/2014)

ABSTRACT. The normal contact stiffness between two polymer blocks with nominally flat surfaces in contact is investigated. Contact stiffness is experimentally determined on a tension-compression machine at small loading steps from zero to about 15 kN. The contact stiffness of steel specimens with the same dimensions as those of the polymer blocks is also investigated to examine the differences between polymers and metals. The three-dimensional surface parameters of the samples are obtained by using an optical profiler. The experimentally measured contact stiffness of Nylon shows a trend similar to that of steel, whereas Teflon and Polyimide show different trends. This discrepancy is shown to be related to the non-homogeneous distribution of surface summits on the contact area. Such a distribution may reduce the real elastic contact area, which in turn changes the surface condition from a rough to smooth contact.

Keywords: contact stiffness, polymer, elastic contact area, surface roughness

Nomenclature

K_B	axial stiffness of upper or lower block
K_m	total measured contact stiffness
K_n	normal contact stiffness between contact pairs
n	number of peaks over surface area of contact
S_a	root mean square (r.m.s.) parameter corresponding to center-line average
S_{ds}	summit density (the number of summits per unit area that make up the surface).
S_q	r.m.s. roughness evaluated over the complete 3D surface
S_{sc}	is the mean summit curvature comprising the summits found for the S_{ds} calculations
s	normalized coordinate (height/σ)
N	normal load
β_1, β_2	average radii of asperities on upper and lower surfaces, respectively
β	effective radius of asperities
η	density of asperities per unit area
ν_1, ν_2	poisson ratios for upper and lower surfaces, respectively
σ	standard deviation of height distribution of asperities

1. Introduction

Flat surfaces are inherently rough because surface roughness and irregularities inevitably arise during manufacturing processes. Many investigations on the contact stiffness characteristics of nominally flat surfaces have been carried out and reported in the literature [1-10]. The principal experimental technique used to determine the normal contact stiffness of nominally flat surfaces is based on the measurement of deformation between two flat specimens under different normal loads [6-8]. The two specimens are pressed together by a normal force and the deformation of asperities is recorded by an electric micrometer or the stylus of a profilometer. The results obtained from this typical setup are refined by means of finite element software to eliminate the effect of deformation of parts of the test machine itself. The investigation of contact stiffness has been made using ultrasonic waves [9-12] to avoid such drawback.

The aim of the present paper is to extend the measurement of normal contact stiffness from metal to polymer pairs with flat surfaces. Polymer materials are widely used in replication technologies. Recently, different methods such as polymer imprinting, casting, hot embossing, and injection molding have been successfully used for polymer replication of different surface structures with nanometer-scale elements [13, 14]. Some comprehensive conclusions regarding the surface and interface properties have been presented [15]. To determine the apparent elastic moduli over 5 to 200 nanometers from the free surface of amorphous polystyrene, some recent advances in contact deformation have been applied [16], where the apparent stiffness of the surface under contact was found to exceed that of the bulk by up to 200% independent of processing scheme, macromolecular structural characteristics, or relative humidity. A 3-D semi-analytical contact model for viscoelastic materials has been used [17] to simulate the contact between a polymethyl methacrylate (PMMA) substrate and a rigid sphere driven by step, ramped, and harmonic normal loads. Approximate closed-form equations for rate-dependent normal and tangential contact forces on a statistical rough surface have been proposed [18]. The tangential contact stiffness between two elastic bodies made of polyvinyl chloride (PVC) and having nominally flat surfaces has been investigated [19]. Shi et al. [20] conducted an extensive study of the normal contact stiffness on unit area of a mechanical joint surface considering perfectly elastic elliptical asperities. Starzynski and Buczkowski [21] studied ultrasonic measurements of the contact stiffness between rough surfaces. Dickrell and Sawyer [22] conducted an extensive study of lateral contact stiffness and the elastic foundation. Recently, Prodanov et al. [23] showed that few parameters suffice to determine many important interfacial properties by combining dimensional analysis and numerical simulation

2. Experimental Technique

The experimental technique used in this work is based on the measurement of the elastic deformation between two flat specimens under different normal loads [1-8]. Table 1 shows the geometrical dimensions for the three polymer specimen pairs and steel specimen pair tested. Nylon is selected as a thermoplastic because it resists abrasion and is self-lubricating, whereas Polyimide is selected as a thermoset resin for its thermal stability, good chemical resistance, and excellent mechanical properties. Teflon (PTFE) is selected as a fluorocarbon because it is hydrophobic (neither water nor water-containing substances wet PTFE) and has one of the lowest coefficients of friction against any solid.

For every specimen pair, their flat surfaces are brought into contact and compressed together under normal loads applied by using an MTS material testing machine (tension-compression machine).

Table (1). Sample Dimensions.

Specimen	Teflon (PTFE)	Polyimide	Nylon	Steel
Dimensions	ϕ 50×40 mm	ϕ 50×40 mm	31×31×31 mm	32×32×32 mm

2.1 Predicting the contact stiffness of polymer contact pairs

The measured normal stiffness K_m of the contact pairs due to normal loading consists of two main components (Figure 1):

i. Material axial stiffness K_B.

ii. Normal contact stiffness K_n due to elastoplastic deformation of encountered asperities.

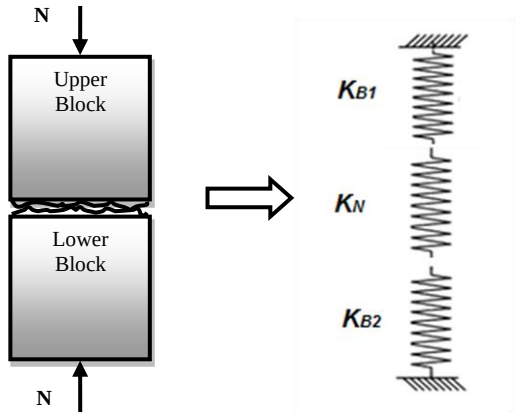

Fig. (1). Modeling of contacting specimen pair

Applying normal force N, the axial stiffness K_B of one block can be calculated as:

$$K_B = \frac{EA}{l_0} \tag{1}$$

According to Figure 1, if the two blocks are physically identical, the total measured stiffness K_m of the contact pairs is given as:

$$\frac{1}{K_m} = \frac{1}{K_{B1}} + \frac{1}{K_n} + \frac{1}{K_{B2}} = \frac{2}{K_B} + \frac{1}{K_n}$$

$$K_n = 1 \Big/ \left(\frac{1}{K_m} - \frac{2}{K_B} \right) \tag{2}$$

Knowing the modulus of elasticity E of the contact pairs, K_B can be obtained from Eq. (1). For example, the modulus of elasticity of E = 0.4 GPa for Teflon results in an axial stiffness K_B of 24.5 MN/m for one Teflon specimen. However, a better way to measure K_B is to compress one element of the specimen pair by using an MTS machine, as shown in Figure 2.

(a) **(b)**

Fig. (2). Compression of Teflon (PTFE) specimen pair. (a) Measurement of axial stiffness K_B and (b) measurement of total stiffness K_m.

3. Results

Figure 3 shows the measured load-displacement curve of a single Teflon specimen. It shows that $K_B \cong 25$ MN/m, which is almost exactly the value computed above by using Eq. (1).

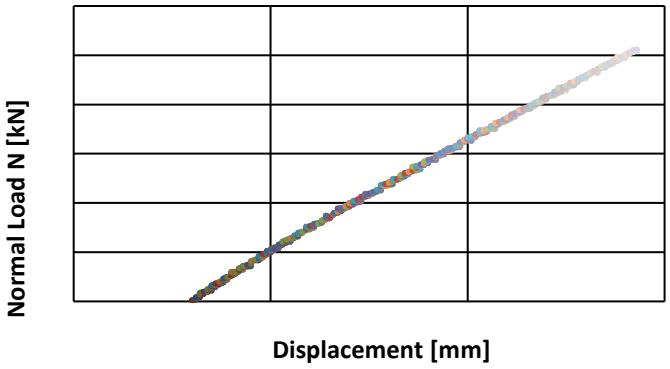

Fig. (3). Measured load-displacement curve of single Teflon specimen

3.1 Measured total stiffness K_m

The contact surfaces of either polymer or steel pairs are compressed by using an MTS machine at a loading rate of 1.0 N/s (Figure 2(b)). The load-displacement curves of the three polymer specimen pairs and steel specimen pair are shown in Figures 4–7.

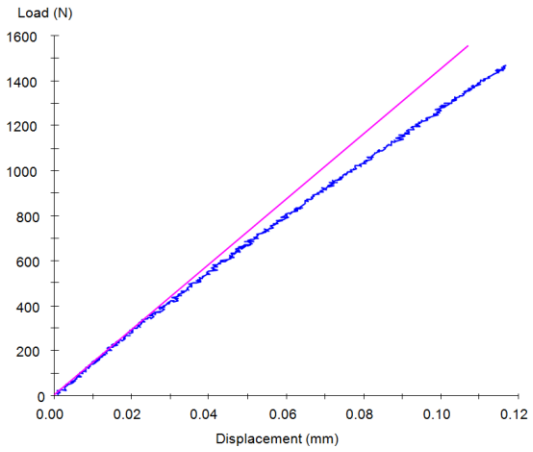

Fig. (4). Experimental load-displacement curve of Teflon specimen pair

Although the total deflection is small, Teflon displays elastomeric elasticity without any significant effect of the roughness of contacting surfaces on this total deformation. In contrast, the elastic deformation behavior of Polyimide and Nylon shown in Figures 5 and 6, respectively, is similar to that of steel (shown in Figure 7), where the initial deformation exponentially increases with the applied normal load.

Subsequently, the load–displacement trend becomes linear. The total stiffness of contact specimen pairs, which is represented by the slope of these curves, increases monotonically with the normal load.

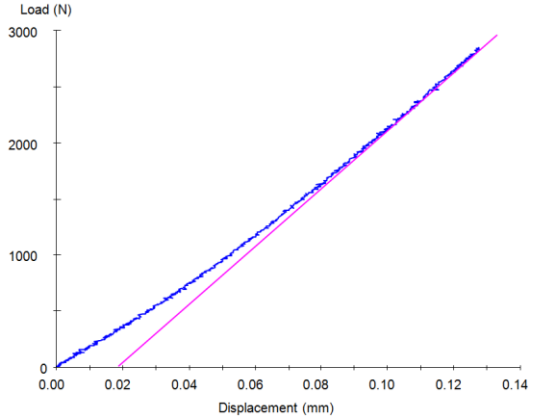

Fig. (5). Experimental load-displacement curve of Polyimide-6 specimen pair

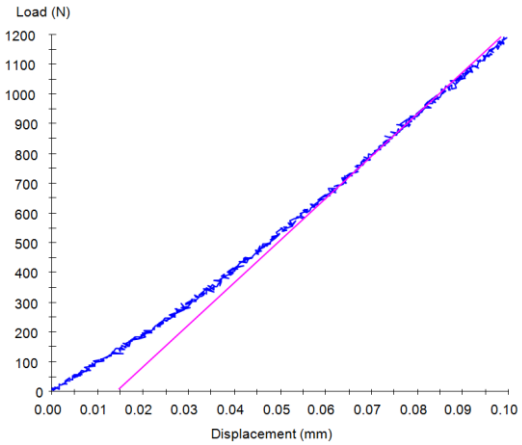

Fig. (6). Experimental load-displacement curve of Nylon specimen pair

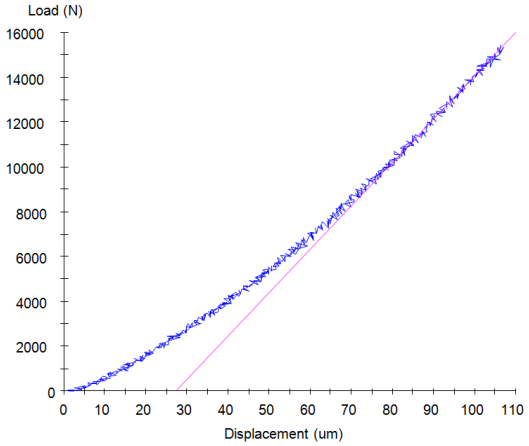

Fig. (7). Experimental load-displacement curve of steel specimen pair

Except for the Teflon specimen pairs, all measured curves in Figures 5–7 show the same trend of variation of displacement with the applied normal load. The slope of the load-deflection of viscoelastic materials is known to increase with the shear rate. However, contact testing of Teflon at a lower loading rate reveals a slightly different trend. Figure 8 shows the load-displacement curve of Teflon at a load rate of 0.05 N/s.

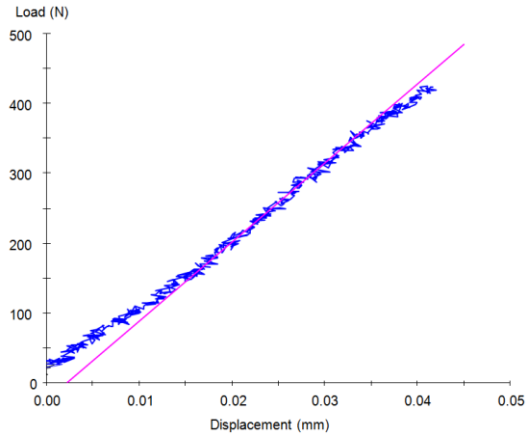

Fig. (8). Experimental load-displacement curve of Teflon specimen pair (load rate, 0.05 N/s).

A comparison between the trends for Teflon at two different rates of the applied normal load is given in Figure 9.

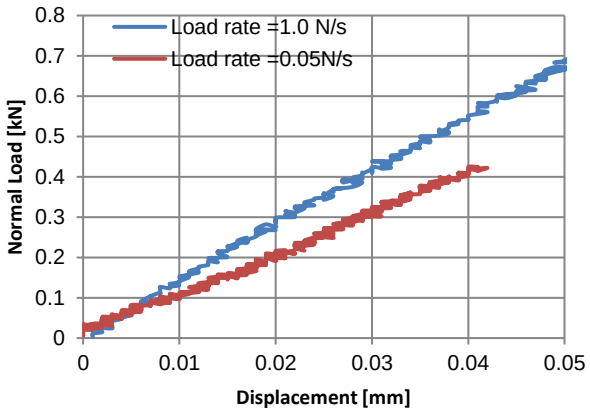

Fig. (9). Effect of load rate on the load-displacement curve of Teflon specimen pair.

3.2 Measured Normal Contact Stiffness K_n

The experimental total stiffness K_m is obtained by using curve-fitting of the load-displacement relationship shown above and then taking the first derivative of the load-displacement curves. Subsequently, the normal contact stiffness K_n is obtained from the derived curve K_m and Eq. (2). Figures 10–13 show the total measured stiffness K_m and the corresponding normal contact stiffness.

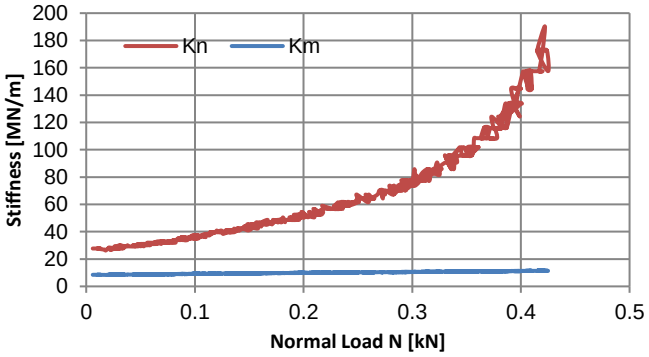

Fig. (10). Variation of the predicted normal contact stiffness of Teflon specimen pair with applied normal load.

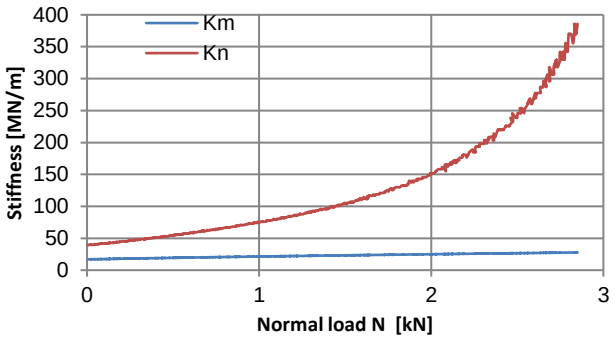

Fig. (11). Variation of the predicted normal contact stiffness of Polyimide specimen pair with applied normal load.

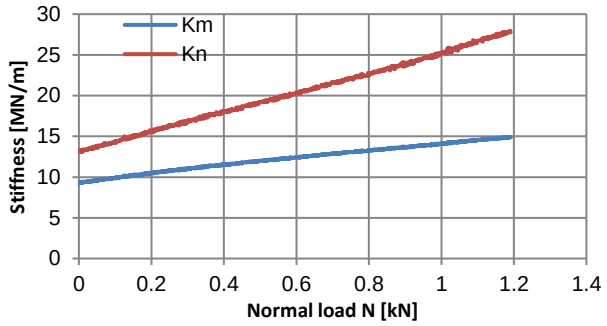

Fig. (12). Variation of the predicted normal contact stiffness of Nylon specimen pair with the applied normal load.

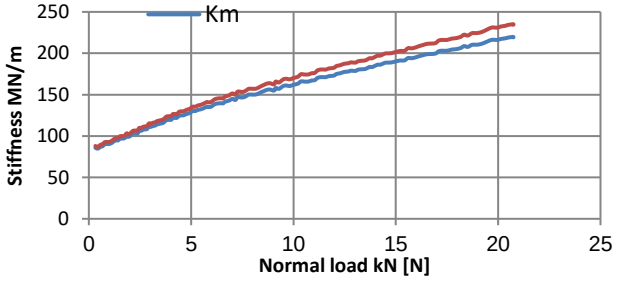

Fig. (13). Variation of the predicted normal contact stiffness of Steel specimen pair with the applied normal load.

3.3 Polymer Surface Topography

Topographical measurement of the polymer surfaces are conducted by using a 3D optical profiler (contour GT), as shown in Figure 14. Polymer surfaces should ideally be scanned with a 10× lens camera by using vertical scanning interferometry (VSI). The measured area is meshed into 4 areas where the dimensions of the scanned subarea are 0.8448 μm × 0.6335 μm. The surface parameters used for contact stiffness calculation are included in the height and hybrid S-parameters. Tables 2–5 show these measured surface parameters for the tested polymer pairs as well as the steel pair.

Fig. (14). Optical scan of Teflon specimen by using GT Contour profiler

Table (2). 3D Surface Parameters of Teflon PTFE specimen pair

	S Parameters (Height)		S Parameters (Hybrid)		Mechanical properties	
	S_a (nm)	S_q (nm)	S_{ds} (1/μm^2)	S_{sc} (1/nm)	$E_1 = E_2$ [GPa]	$\nu_1 = \nu_2$
Upper surface	1050.8	1450	0.0086	0.00128	0.5	0.39
Lower surface	900.5	757.8	0.00953	0.00127	0.5	0.39

Table (3). 3D Surface Parameters of Polyimide specimen pair

	S Parameters (Height)		S Parameters (Hybrid)		Mechanical properties	
	S_a (nm)	S_q (nm)	S_{ds} (1/μm^2)	S_{sc} (1/nm)	$E_1 = E_2$ [GPa]	$\nu_1 = \nu_2$
Upper surface	2720.3	3640	0.00506	0.00102	3.1	0.34
Lower surface	3248.6	4218	0.00421	0.0014	3.1	0.34

Table (4). 3D Surface Parameters of Nylon specimen pair

	S Parameters (Height)		S Parameters (Hybrid)		Mechanical properties	
	S_a (nm)	S_q (nm)	S_{ds} (1/μm^2)	S_{sc} (1/nm)	$E_1 = E_2$ [GPa]	$\nu_1 = \nu_2$
Upper surface	1528.8	2036.18	0.129188	0.01306	2.0	0.46
Lower surface	2149.6	2693.40	0.1359	0.0165	2.0	0.46

Table (5). 3D Surface Parameters of steel pair

	S Parameters (Height)		S Parameters (Hybrid)		Mechanical properties	
	S_a (nm)	S_q (nm)	S_{ds} (1/μm^2)	S_{sc} (1/nm)	$E_1 = E_2$ [GPa]	$\nu_1 = \nu_2$
Upper surface (ground)	46.6	63.5	0.096138	0.0004672	210	0.3
Lower surface (polished)	39.9	54.6	0.00399	0.000023	210	0.3

To correctly assess all tested surfaces, the average values of parametersβ, σ, and η, in addition to the average surface roughness S_a, must be computed from data given in the above tables as follows [24]:

$$S_a = S_{a1} + S_{a2} \tag{3}$$

$$\frac{1}{\beta} = \frac{1}{\beta_1} + \frac{1}{\beta_2} = S_{sc1} + S_{sc2} \tag{4}$$

where

$$S_{sc} = \frac{1}{n}\sum_{1}^{n} \int_{Summit\_y} \int_{Summit\_x} \left[\left(\frac{\partial^2 z(x,y)}{\partial x^2} \right) + \left(\frac{\partial^2 z(x,y)}{\partial y^2} \right) \right] dxdy$$

and

$$\sigma = \sqrt{S_{q1}{}^2 + S_{q2}{}^2} \tag{5}$$

where

$$S_q = \iint z(x,y)^2 \, dxdy$$

and

$$\eta = \frac{S_{ds1} + S_{ds2}}{2} \tag{6}$$

where

$$S_{ds} = \frac{Number\,of \quad peaks}{Measured\,area} \tag{7}$$

Table 6 shows the average surface parameters computed according to the above equations.

Table (6). Surface Parameters of Tested Samples

	S_a (nm)	σ_q (nm)	η (1/μm^2)	β (nm)
Teflon	975	1635	110	784
Polyimide	2984	5571	215.7	413
Nylon	1838.5	3376	7.57	67.7
Steel	43.25	83.7	20	2040.8

Smooth surfaces show very small values of σ_q and η but a large radius β. Inspection of data in Table 6 reveals that Teflon is smoother than Polyimide and Nylon but rougher than steel.

In addition, representative 3-D plots of the scanned surfaces are given in Figures 15–18. For these plots, an additional surface feature that can be investigated is the distribution of surface summits (asperities). The Teflon surface plot in Figure 15 shows limited numbers of randomly dispersed asperities. Many surface measurements of Teflon on the same scale yield no summits, as shown in Figure 16. This suggests that the surface of Teflon is very smooth.

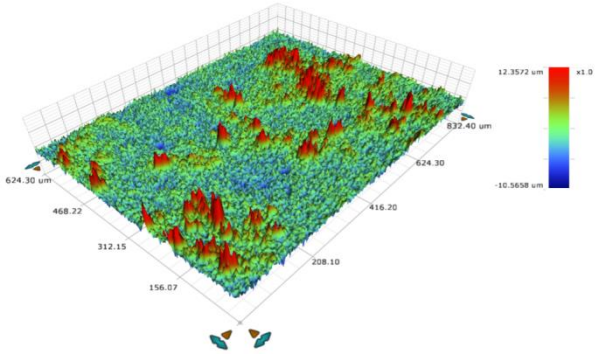

Fig. (15). 3D Surface Plot of Teflon

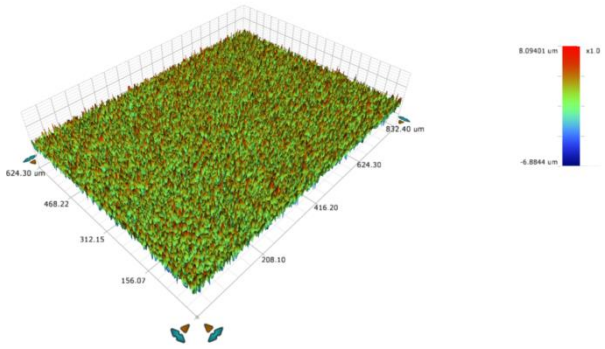

Fig. (16). Teflon 3D Surface Plot with no summits

A lesser discrepancy in surface roughness exists in case of Polyimide, where greater numbers of summits are agglomerated and not randomly dispersed, as shown in Figure 17.

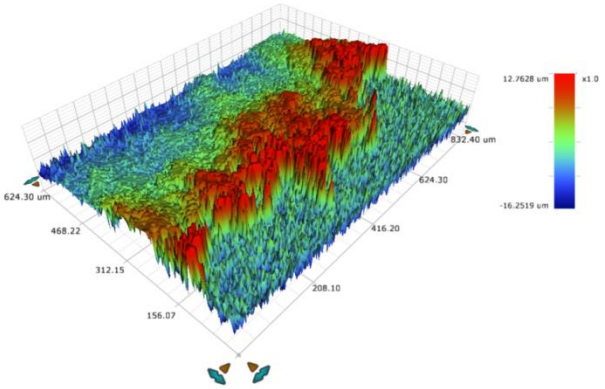

Fig. (17). 3D Surface Plot of Polyimide

In contrast, the typically rough surfaces of Nylon and steel samples can be observed in Figures 18 and 19, respectively. These plots also indicate the typical trends in their values of contact stiffness as a function of the applied normal load.

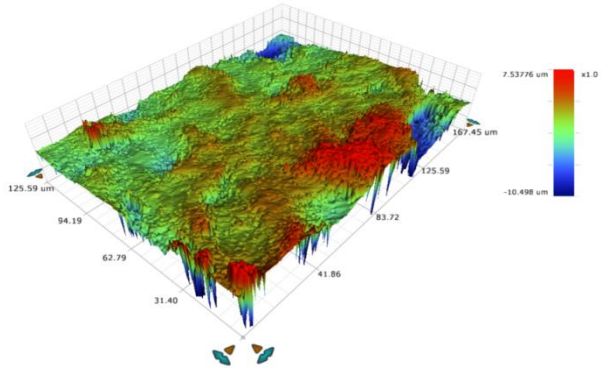

Fig. (18). 3D Surface Plot of Nylon

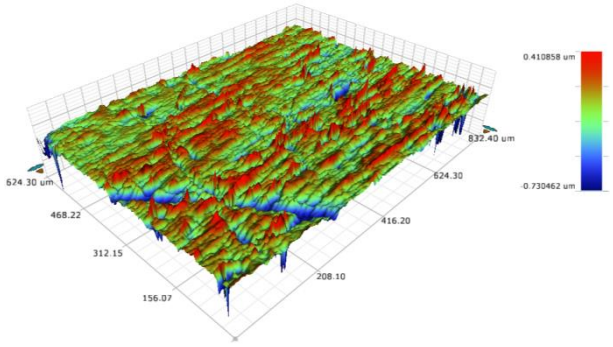

Fig. (19). 3D Surface Plot of Steel

4. Discussion

According to the Greenwood–Williamson theory of contact [25], encountered asperities are assumed to have spherical shapes with mean radius β and heights that follow a Gaussian distribution. As the normal load increases, more and more asperities come to contact, which results in a higher normal contact stiffness. Our experimental results reveal this trend for the compression of Nylon (Figure 18) and steel (Figure 19). In contrast, the contact stiffness trends for Teflon and Polyimide are identical, although they are different from those of steel and Nylon specimen pairs. This can be explained by the particular configuration of their surface topographies, which show nearly smooth (that is, weakly rough) surfaces.

5. Conclusion

Values of normal contact stiffness for three polymer specimen pairs were determined by experimental investigation on a compression-tension machine under different normal loads. All surfaces were measured by using an optical profiler before loading. The material properties of the tested samples used in the investigation and the topographical surface parameters for their contact surfaces were described. 3D representations of the polymer contact surfaces were also shown. Values of axial stiffness for the tested polymer blocks were identified from the measured load-displacement curve by compressing a single polymer block. On the basis of this experimental investigation, some concluding remarks can be summarized as follows:

i. The normal contact stiffness of a Nylon specimen pair shows a trend similar to that of steel, that is, a gradual increase with the normal load, albeit within different ranges of load and displacement for each. This similarity in the trend is related to the homogeneity of their surface topographies.

ii. The compression of contacting surfaces of Teflon or Polyimide results in an elastoplastic deformation of the few dispersed or agglomerated asperities up to a particular load. Beyond this load, no more asperities are in contact and the possibility of smooth flat to flat contact is attained. The particular loads are 0.26 and 1.5 kN for Teflon and Polyimide, respectively. The corresponding values of contact stiffness are 65 and 100 MN/m.

6. References

[1] Thornley, R. H., Connoly R. and Koenigsberger, F., "The effect of flatness of .joint faces upon the static stiffness of machine tool joints," *Proc. Inst. Mech. Eng.*, Vol. 182, No. 1(18), (1967-1968), pp. 271-277.

[2] Dolbey M. P. and Bell, R., "The contact stiffness of joints at low apparent interface pressure," Ann. CZRP (1970).

[3] PaI, D., K. and Basu, S. K., "Surface preparation of machine tool slideways and its influence on the contact stiffness," *Int.*, Vol. 6, No. 5, (1373), pp. 172-180.

[4] Chikate, J. P. and Basu, S. K., "Contact stiffness of machine tool joints," Tribol. Int., Vol. 8, No. 1, (1975), pp. 3-14.

[5] Bush, A.W., Gibson, R.D., and Thomas, T.R., "The elastic contact of a rough surface," *Wear*, 3.5 (1975), pp. 87-111.

[6] Burdkein, M., Back, N., and Cowley, A., "Experimental study of normal and shear characteristics of machined surfaces in contact," *J. Mech. Erg. Sci*., Vol. 20, No. 3, (1978), p. 129.

[7] Chicate, P. and Basu, S. K., "Contact stiffness of machine tool joints," *Tribal. Znt.*, Vol. 8, No. 1, (1975), p. 9.

[8] Tsukada, T. and Anno, Y., "An analysis of the deformation of contacting rough surfaces," *Bull. JSME,* Vol. 15, No. 86, (1972), p. 982.

[9] Dwyer-Joyce, R. S., Drinkwater, B., W. and Quinn, A. M., "The use of ultrasound in the investigation of rough surface interfaces," *ASME Journal of Tribology*, Vol. 123, (2001), pp. 8-16.

[10] Baltazar, A., Rokhlin, S. I. and Pecorari, C., "On the relationship between ultrasonic and micromechanical properties of contacting rough surfaces," *Journal of the Mechanics and Physics of Solids*, Vol. 50, (2002), pp.1397-1416.

[11] Kim, J.-Y., Baltazar, A. and Rokhlin, S. I., "Ultrasonic assessment of rough surface contact between solids from elastoplastic loading-unloading cycle," *Journal of the Mechanics and Physics of Solids*, Vol. 52, (2004), pp. 1911-1934.

[12] Goerke, D. and Willner, K., "Experimental setup for normal contact stiffness measurement of technical surfaces with geometrical irregularities," *Experimental Techniques*, doi: 10.1111/j.1747-1567.2008.00448.x, (2009), pp.46-52.

[13] Gale, M. T., "Replication techniques for diffractive optical elements," *Microelectronic Engineering*, Vol. 34, (1997), pp. 321-339.

[14] Krauss, P. R., Chou, S. Y., "Nano-compact disks with 400 gbit in storage density fabricated using nano imprint lithography and read with proximal probe," *Appl. Phys. Lett.*, Vol. 71, No. 21, (1997), pp. 3174-3176.

[15] Alcoutlabi, M., McKenna, G. B., "Effects of confinement on material behaviour at the nanometer size scale," *J. Phys.: Condens. Matter*, Vol. 17 (2005), pp. R461-R524.

[16] Tweedie, C. A., Constantinides, G., Lehman, K. E., Brill, D. J., Blackman, G. S., Van Vliet, K. J., "Enhanced stiffness of amorphous polymer surfaces under confinement of localized contact loads," *Advanced Materials*, Vol. 19, (2007), pp. 2540-2546, doi: 10.1002/ adma.200602846.

[17] Chen, W. W., Wang, Q. J., Huan, Z., Luo, X., "Semi-analytical viscoelastic contact modeling of polymer-based materials," *Journal of Tribology*, Vol. 133, (2011) /041404-1.

[18] Farhang, K., and Lim, A., "A kinetic friction model for viscoelastic contact of nominally flat rough surfaces," *ASME J. Tribol*, Vol. 129, (2007), pp. 684-688.

[19] Piscan, I., Ompusunggu, A. P., Janssens, T., Redincea, N., "Theoretical and Experimental Contact Stiffness Characterisation of Nominally Flat Surfaces," *Applied Mechanics and Materials*, Vol. 186, (2012), pp. 107-113.

[20] Shi, J. P., Ma, K., Liu, Z. Q., "Normal contact stiffness on unit area of a mechanical joint surface considering perfectly elastic elliptical asperitiesm," *J. Tribol*, 134 (3):031402-031402-6, doi: 10.1115/1.4006924, (2012).

[21] Starzynski, G., Buczkowski, R., "Ultrasonic measurements of contact stiffness between rough surfaces," *J. Tribol*, TRIB-13-1225, doi: 10.1115/1.4027132, (2014).

[22] Dickrell, D. J., Sawyer, W. G., "Lateral contact stiffness and the elastic foundation," *Tribology Letters*, Vol. 41, No. 1, (2011), pp. 17-21.

[23] Prodanov, N., Dapp, W. B., Müser, M. H., "On the contact area and mean gap of rough, elastic contacts: dimensional analysis, numerical corrections, and reference data," *Tribology Letters*, Vol. 53, No. 2, (2014), pp. 433-448.

[24] Greenwood, J. A., Williamson, J. B. P., "Contact of nominally flat surfaces," *Proceedings of the Royal Society of London*, Vol. A295, (1966), pp. 300-319.

[25] Sherif, H. A., "Parameters affecting contact stiffness of nominally flat surfaces," *Wear*, Vol. 145, (1991), p. 113.

صلابة التلامس لعينات من البوليمر ذات الأسطح المستوية

فهد عبدالرحمن المفضي

كلية الهندسة – قسم الهندسة الميكانيكية، جامعة القصيم

ص.ب. ٦٦٧٧ - بريدة، القصيم ٥١٤٥٢ – المملكة العربية السعودية

almufadi @qec.edu.sa

(قدم للنشر في ٢٠١٤/٢/٢٣؛ وقبل للنشر في ٢٠١٤/٤/١٣)

ملخص البحث. اهتم البحث بالتحقق من صلابة التلامس العمودي بين كتلتين من البوليمر في الاسطح المستوية. تم ايجاد صلابة التلامس معملياً من خلال ماكينة الضغط والشد بتحميل قوة صغيرة جدا من صفر إلى ما يقارب ١٥كيلو نيوتن. تم فحص صلابة التلامس لعينات من الصلب لها نفس ابعاد كتل عينات البوليمر لدراسة الاختلافات بين البوليمر والمعادن.

تم ايجاد عوامل المتغيرات للسطح ثلاثي الابعاد للعينات باستخدام جهاز التعريف البصري. من خلال التجارب المعملية تم قياس صلابة التلامس لعينات النايلون والتي اظهرت اتجاها مماثلاً لتلك التي من الصلب بينما وجد اتجاهات مختلفة للتفلون والبوليمر .هذا الاختلاف يعزى الى علاقة التوزيع الغير متجانس لقمم الاسطح في المناطق المتلامسة. مثل هذا التوزيع قد يقلل من منطقة المرونة الحقيقية للتلامس ، وهذا بدوره يغير حالة السطح من التلامس الخشن الى الناعم.